

Photoemission Studies on $\text{Bi}_2\text{Sr}_2\text{Ca}(\text{Cu}_{1-x}\text{Zn}_x)_2\text{O}_{8+\delta}$ - Electronic Structure Evolution and Temperature Dependence

P.J. White⁽¹⁾, Z.-X. Shen⁽¹⁾, D.L. Feng⁽¹⁾, C. Kim⁽¹⁾, M.-Z. Hasan⁽¹⁾, J.M. Harris⁽¹⁾, A.G. Loeser⁽¹⁾, H. Ikeda⁽²⁾, R. Yoshizaki⁽²⁾, G.D. Gu⁽³⁾, N. Koshizuka⁽⁴⁾

⁽¹⁾ *Department of Applied Physics and Stanford Synchrotron Radiation Laboratory, Stanford University, Stanford, CA 94305-4045*

⁽²⁾ *Institute of Applied Physics and Cryogenics Center, University of Tsukuba, Tsukuba, Ibaraki 305 Japan*

⁽³⁾ *School of Physics, The University of New South Wales, PO Box 1, Kensington, N.S.W., Australia 2033*

⁽⁴⁾ *Superconductivity Research Laboratory, ISTEC, 10-13 Shimonome, 1-Chome, Koto-Ku, Tokyo 135, Japan*

An angle resolved photoelectron spectroscopy study was conducted on $\text{Bi}_2\text{Sr}_2\text{Ca}(\text{Cu}_{1-x}\text{Zn}_x)_2\text{O}_{8+\delta}$. A small amount of Zn substitution for Cu almost completely suppresses the otherwise sharp spectral peak along the $(0,0)$ to (π, π) direction in $\text{Bi}_2\text{Sr}_2\text{Ca}(\text{Cu}_{1-x}\text{Zn}_x)_2\text{O}_{8+\delta}$, while superconductivity with T_c as high as 83K survives. This behavior contrasts markedly from that seen in cases where the impurities are located off the CuO_2 plane, as well as when the CuO_2 planes are underdoped. This effect is also accompanied by changes of low energy excitations at $(\pi, 0)$, near the anti-node position of the $d_{x^2-y^2}$ pairing state. With Zn doping the size of the superconducting gap is significantly suppressed, the width of the quasiparticle peak in the superconducting state becomes wider, and the dip at higher binding energy is diminished. In addition, enhanced temperature induced spectral changes also occur. We show intriguing systematic lineshape changes with temperature that persist to a very high energy scale - a result consistent with the idea that Zn enhances the local charge inhomogeneity.

PACS:71.20.-b,71.27.+a,74.25.Jb

I. INTRODUCTION

Impurity doping has been a very effective tool to probe the properties of cuprate superconductors. In particular, Zn substitution of Cu in the CuO_2 planes is known to suppress T_c [1] - [6]. An extensive amount of experiments has been conducted to understand the effect of Zn doping, including specific heat, microwave, NMR, μSR , optical, neutron, and tunnelling experiments [7] - [20]. Transport and microwave experiments indicate that Zn is a very strong scatterer, resulting in a strong increase in the residual resistivity in the plane [3] [4] [12]. A similar conclusion was drawn from μSR experiments, which also found that Zn suppresses the superfluid density [15]. Specific heat, transport, and optical experiments indicate that Zn doping alters the residual density of states and affects the low energy charge dynamics [10] - [13] [21]. NMR and neutron experiments generally show that Zn introduces low lying excitations in the spin channel [16] - [19] and dramatically affects the dynamical spin fluctuations. In particular, the NMR experiments show that Zn induces local magnetic moments in the normal state that do not otherwise show local moment behavior.

More recently, Zn doping was also found to enhance the T_c suppression and other anomalies near $\frac{1}{8}$ doping in $\text{La}_{2-x}\text{Sr}_x\text{CuO}_4$ (LSCO), $\text{YBa}_2\text{Cu}_3\text{O}_7$ (YBCO), and Y doped $\text{Bi}_2\text{Sr}_2\text{CaCu}_2\text{O}_{8+\delta}$ (Bi2212) [22]. This latter result has been speculated to be due to the charge stripe instability [22], similar to a possible interpretation of neutron data from LSCO. In addition, a neutron scattering experiment has shown two aspects of Zn doping. First, it found

that Zn shortened the correlation length of the static spin density wave [20]. Second, it found that the Zn shifted the spectral weight to lower energy, a fact consistent with the idea that Zn serves to stabilize a short range order incommensurate spin density wave state which might otherwise be purely dynamic [16] [20].

This issue of microscopic phase separation is of current interest. Based on incommensurate neutron scattering data from LSCO (recently also observed in YBCO [23]), it has been proposed that the cuprates develop stripes at low temperature in certain doping regimes [19] [20]. Here the stripes refer to microscopically phase separated insulating and metallic regions forming spin and charge ordered one-dimensional structures [24] - [30]. While the interpretation of neutron data is plausible, the experimental evidence for charge ordering remains elusive at present. Except for the case of Nd doped LSCO, no evidence of charge ordering has been detected. Zn doped Bi2212 may be a good system for an angle resolved photoelectron spectroscopy (ARPES) investigation of this issue. First, Zn doping is found to enhance the T_c suppression and other anomalies near $\frac{1}{8}$ doping in LSCO [22], YBCO [23], and Y doped Bi2212 [31]. The $\frac{1}{8}$ anomaly is thought to be associated with the stripe instability [19]. Second, from what we will show later, Zn impurities dramatically alter the electronic structure along the $(0,0)$ to (π, π) line. This data can be rationalized by the fact that Zn induces an antiferromagnetic region around it and enhances the local charge inhomogeneity.

By using ARPES, we will explore these aspects in detail. Over the last decade ARPES has played an im-

portant role in advancing our understanding of the low energy single particle excitations in these novel superconductors, starting with the observation of band like features [32]. Most notably, ARPES facilitated the observation of the d-wave superconducting gap structure as well as the normal state pseudogap [33] [34] [35] [36]. Several groups have attempted to study the impurity doping effects of the electronic structure using ARPES. Quitmann *et al.* [37] have performed room temperature ARPES of Ni and Co doped Bi2212 to address the changes of the electronic structure in the normal state but not the changes in the superconducting state. Our experiments on Bi2212 will address both the normal and superconducting states. Gu *et al.* [38] have attempted to study Zn and Co doped YBCO for which the superconducting property of the CuO₂ planes is complicated by the surface chain signal [39]; Bi2212 lacks the surface chain complication of YBCO.

II. EXPERIMENTAL

Single crystals of Bi₂Sr₂Ca(Cu_{1-x}Zn_x)₂O_{8+δ} (Zn doped Bi2212, x=0.006,0.01) were prepared using a traveling solvent floating zone method [40] [41]. These crystals were characterized according to T_c and the Zn concentration, which was determined by electron probe microanalysis (EPMA). The crystals were grown under the nominal condition to produce optimal doping, with T_c of the Zn doped samples ranging from 83K to 78K. The transition widths vary from 3-5K according to susceptibility measurements, indicating the high quality of these crystals. The single phase of the samples was verified by X-ray scattering. X-ray rocking curves indicate that the crystalline quality of the Zn doped Bi2212 is comparable to that of the pure Bi2212; the presence of stacking faults was checked by taking the rocking curves of the (0,0,ℓ) X-ray diffraction peaks and the results were comparable between pure Bi2212 and our Zn doped Bi2212 [40]. In addition, Laue back scattered X-ray diffraction was done for alignment purposes and no difference was detected between the standard and the Zn doped sample. In this paper, data from 3 samples of pure Bi2212 are presented with T_c≈91K, 89K and 88K. The former two reveal themselves to be typical samples of high quality, but the last one with a critical temperature of 88K exhibits behavior between the ones closer to optimal doping and the ones doped with Zn. Therefore, we conjectured that the 88K sample had some unknown impurities. Attempts were made to determine the stoichiometry more precisely via EPMA, but owing to the number of species in the compound and the low concentration of the impurity, this was difficult with conventional means. While this may seem strange to include, it is nevertheless presented to make a connection to our previously published results [42] and to provide continuity of our work. This

paper is also an homage to the previously neglected subtleties on our part associated with this kind of doping in Bi2212. Therefore, we elucidate our old results in light of our new findings.

Data in Figs. 1, 2, 3, 4, 5 were recorded with a Vacuum Science Workshop analyzer attached to beamline 5-3 of the Stanford Synchrotron Radiation Laboratory (SSRL). The total energy resolution was typically 35meV and the angular resolution was ±1°. The nominal chamber pressure during the measurement was 2-3x10⁻¹¹ torr and the photon energy used was 22.4eV. At this photon energy an ARPES spectrum mimics the spectral function, A(**k**,ω) [43], weighted by the appropriate factors, such as matrix elements, the Fermi function, etc. The ARPES spectra in the remaining data were recorded with a Scienta analyzer attached to beamline 10 of the Advanced Light Source (ALS). The total energy resolution was typically 15meV and the angular resolution was ±0.15° with the spectrometer operating in angle mode. The nominal chamber pressure was 6x10⁻¹¹ torr and the photon energy used was 25eV. Spectra from SSRL were taken within 10-12 hours of cleaving so as to minimize aging effects as previously reported [33] [44]. Spectra from ALS were taken within a shorter time to compensate for additional aging caused by the higher photon flux. With the SSRL apparatus, we can only take selected **k** points in order to have spectra with low enough statistical noise to identify subtle changes in the lineshape. With the ALS apparatus we can take about 40 spectra at the same time with 0.15°-0.3° spacing. The flatness of the surfaces of the pure and Zn doped samples was verified by laser reflection patterns after the samples were cleaved *in situ*. Fermi levels were determined by a gold reference sample in electrical contact to the samples.

III. ELECTRONIC STRUCTURE EVOLUTION

In this section we report detailed results of ARPES on the nature of the Zn doping effect on the electronic structure of the Zn doped Bi2212 system. We found significant changes in the electronic structure near the Fermi level with a small amount of Zn doping. Along the (0,0) to (π,π) direction, Zn doping essentially wipes out the otherwise well defined spectral peak [45] in samples with T_c as high as 83K. This behavior contrasts strongly to the case where scattering impurities are located off the CuO₂ plane as well as to the case of an underdoped CuO₂ plane. Zn doping also causes systematic changes in data near (π,0), which is close to the anti-node region of the d-wave pairing state. Indeed, the superconducting gap is decreased as one would expect from pair breaking considerations. At the same time, the dip seems almost gone in Zn doped Bi2212. This suggests an interesting evolution of the (π,0) superconducting spectrum as the traditionally two distinct features (the broad incoherent peak and

the sharp spectral peak) seem to evolve simultaneously with Zn doping.

A. Experimental Observation

Fig. 1 presents ARPES data at selected \mathbf{k} -space points along $(0,0)$ to (π,π) for pure, Zn doped, Dy doped and underdoped samples. Two sets of data from the pure and the Zn doped samples are shown to illustrate the reproducibility. These points were chosen for their proximity to the Fermi surface and were spaced sufficiently in momentum to reveal the behavior of the Fermi level crossing. For data from pure sample in Fig. 1a-b, we see a relatively sharp feature disperse across E_f in the expected way. As the peak gets closer to the Fermi level, it apparently narrows in width and, at some point, loses intensity until it ultimately vanishes. This observation is consistent with previous work [32] [34] [35] [36], and much of the peak width is attributable to angular and energy resolutions. This general behavior is qualitatively what one expects of a quasiparticle. For data from the Zn doped samples from Fig. 1c-d, the dramatic difference is readily apparent. The spectral peak is wiped out with no sharp feature seen at the expected crossing or before it [46]. (We note in Fig. 1d that the peak is not recovered upon cooling.) For comparison, Fig. 1e-f reproduces our results from two underdoped samples in similar \mathbf{k} -space locations [34]. The underdoping in these samples (T_c near 65K for both) was achieved either by removing oxygen or by substituting 10% Ca by Dy. In both cases the feature along ΓY remains fairly sharp; this contrasts strongly with data from the Zn doped samples in Fig. 1c-d. For the 10% Dy doped sample there is the additional effect of scattering by Dy impurities, whose concentration is much higher than that of the Zn impurities. It is clear that the Zn impurities in the CuO_2 plane did far more damage to the quasiparticle peak than the more highly concentrated Dy impurities, which are located in the Ca plane sandwiched by the CuO_2 planes.

Fig. 2 shows the $(\pi,0)$ spectra of the pure and the Zn doped samples and reproduces previously published results on overdoped and underdoped samples for comparison. Unlike the ΓY line as shown in Fig. 1, the normal state spectra of the pure and Zn doped samples are similar in this region of \mathbf{k} -space. Both samples show very sharp peaks in the superconducting state. The fact that one can see such a sharp peak below T_c in Zn doped samples gave us confidence on the intrinsic nature of the very broad feature in Fig. 1c-d. It is possible that a disordered surface can produce the effect seen in Fig. 1c-d, however the coexistence of a disordered surface and the sharp feature seen in the data at $(\pi,0)$ is unlikely.

There are several subtle but important differences between the $(\pi,0)$ superconducting spectra for the pure and Zn doped samples. Readily apparent is the fact that

there is virtually no dip at the higher binding energy side of the sharp peak in the Zn doped samples, whereas the dip is clearly visible in the pure sample as found before [47] [48]. The superconducting quasiparticle peak is also broader in the Zn doped sample, implying a stronger scattering rate. In the Zn free sample, the peak width is resolution limited. While the spectral weight of the Zn free sample is balanced above and below T_c , the spectral weight of the Zn doped sample is increased at lower temperature because of the sharp peak's development. Two changes in the spectra contribute to this imbalance: the dip no longer exists and the peak is significantly broadened, even though it has the same relative maximum. The sum rule of $A(\mathbf{k},\omega)$ requires spectral weight to come from other locations in energy and/or momentum space. We will address this point later.

Another significant observation in Fig. 2a is that the sharp peak in the Zn doped sample shifts to lower binding energy as compared to that of the Zn free sample. This can be interpreted as the size of the superconducting gap being suppressed in the Zn doped sample. In the literature, the size of the energy gap in photoemission is often characterized by the position of the leading edge midpoint in the spectra recorded at the underlying Fermi surface [33] [34] [35] [36]. In this case, because the peak is appreciably broadened in the Zn doped sample, the leading edge analysis is not ideal. We use the quasiparticle peak position as a way to characterize the gap. Here, we use the $(\pi,0)$ peak even though it is not exactly at the Fermi crossing. However, since the band dispersion is very flat in this region, we can use it to track the relative change in the gap size.

The relative changes of the peak in Fig. 2a suggest the superconducting gap is suppressed in the Zn doped samples. Note the difference in the rate of Δ suppression and T_c suppression as a function of Zn doping. It is clear that the gap is severely suppressed in the Zn doped samples, given the modest T_c decrease at this doping level. This was consistent with an earlier conclusion that T_c and gap are not directly related energy scales [24]. A possible scenario is that T_c is not limited by pairing strength but by phase fluctuation effects [49] [50] [51]. It is also worth noting that the normal state spectrum at $(\pi,0)$ of the Zn doped sample is cut off by the Fermi function, ruling out the existence of the normal state pseudogap. This is not the case for Zn free Bi2212 in Fig. 2a. This finding can be interpreted as Zn doping suppressing the pseudogap or creating low lying excitations inside the gap as reported by other experiments [17] [18].

Summarizing data from Figs. 1 and 2, we observed correlated changes of the electronic structure as a function of Zn doping: the strong suppression of the quasiparticle along the ΓY line; the suppression of the superconducting gap; the broadening of the superconducting peak and the suppression of the dip near $(\pi,0)$.

B. Discussion of Electronic Structure Evolution Results

The experimental data presented raise several interesting points about impurity doping in the cuprates. The first and foremost has to do with whether the conduction mechanism can be described by quasiparticle dynamics. The dramatic differences in the ARPES data of Fig. 1c-d with a small amount of Zn doping is unexpected from the doping dependence studies of other materials. Photoemission is a signal averaging experiment and is usually quite insensitive to a small amount of doping change, unlike the case here. In transition metal oxides one usually sees only subtle changes with doping variation up to 10-20% [52]. In ordinary metals like Cu or Al the spectra do not change with a very small amount of impurities. This is not the case for Zn doping; the spectra change dramatically. The fact that the change in the Zn spectra in the normal state was consistent with the change in the superconducting state gave us confidence on the intrinsic nature of this effect (again we note that the very sharp peak below T_c at $(\pi, 0)$ shows it was not due to a contaminated surface). The magnitude of the change with a relatively small amount of Zn suggests the system may be very close to a certain instability, and the effect of the Zn impurity is amplified by this intrinsic instability. In Zn free samples the sharp, dispersive feature along the ΓY direction resembles what one would expect from quasiparticles with well defined \mathbf{k} , although the feature is still too broad for this description. On the other hand, Zn doped Bi2212 showed that there is no quasiparticle with well defined \mathbf{k} at all in this direction. Given the modest change of T_c , the change seen in Fig. 1c-d is quite remarkable. It suggests that normal state quasiparticles with well defined momenta are not essential for superconductivity. The observed change of the low energy electronic structure in Fig. 1c-d is consistent with reports from other experiments. NMR, specific heat, microwave, optics, and transport experiments indicate that Zn doping alters the residual density of states [10] - [13] [21] and affects the low energy and spin dynamics [15] - [19]. The \mathbf{k} -resolved information from ARPES is new.

To emphasize the peculiar effect of only a tiny amount of Zn (0.6%, average concentration), we wish to examine what one would expect from simple considerations. Naively, one would think that Zn doping causes scattering in the CuO_2 plane, and this would cause an angular averaging effect; this is similar to the scattering of an incident electron with wavenumber \mathbf{k} by an impurity and mixing with the scattered spherical wave, which is made of a range of \mathbf{k} . To mimic this process we averaged the spectra from the six angles in Fig. 1a and still obtained a reasonably sharp peak (uppermost curve of Fig. 1a). As parallel cuts are similar in the nearby regions, inclusion of these cuts in the averaging process would give a simi-

lar effect to what we have done here. The averaged data still had a sharper structure than those in Fig. 1c-d. Considering the Zn doping is only 0.6%, the scattering effect would be much less than the averaging process as we have done here even if Zn acts as a scatterer. Therefore, the notion of Zn being a simple scatterer seems insufficient to explain the effect seen in Fig. 1c-d. An alternate hypothesis is required. It may be that the Zn impurities induce some collective effects like the ones suggested by neutron experiments. One collective effect is that Zn impurities induce long range antiferromagnetic order that co-exists with the spin-Peierls transition seen in $\text{Cu}_{1-x}\text{Zn}_x\text{GeO}_3$ [53] [54] [55].

Another is that the Zn impurities may pin the dynamical stripes [16] [19]. We will now explore whether this idea provides a self consistent explanation to our data. Specifically, we want to see whether the data are compatible with the idea that Zn impurities pin the dynamical stripes. There are two reasons for us to consider this possibility. The first has to do with transport experiments at $\frac{1}{8}$ doping [22]. It has been strongly suggested that the T_c suppression and other transport anomalies at $\frac{1}{8}$ doping are related to the stripe instability [19]. The work on Zn-Y doped Bi2212 is particularly relevant to our discussion here [31]. In Zn doped cases (2-3%), it is found that the electrical resistivity and thermoelectric power exhibit less metallic behavior than usual near a doping level of $\frac{1}{8}$. At the same time, T_c 's for samples near a doping level of $\frac{1}{8}$ are also anomalously suppressed. These results suggest that the Zn doped Bi2212 system has certain similarity to the LSCO system where data are interpreted as possible evidence that Zn pins the dynamical stripes. The second reason concerns results from neutron experiments. Recent neutron scattering data from Zn doped LSCO indicate that Zn doping shifts the spectral weight of the incommensurate peaks at $(\pi, \pi \pm \delta\pi)$ to lower frequencies [16]. As the incommensurate peaks are interpreted as scattering from dynamical stripes [19], the downward shift of spectral weight has been interpreted as stabilization of the dynamic stripes [16]. On the other hand, it is also found that Zn broadened the incommensurate neutron peak, which indicates that Zn doping disrupts the long range order and shortens the correlation length. Hence, it appears that a random distribution of Zn impurities shortens the long range correlation but stabilizes the short range correlation which would otherwise be more dynamic [19].

Now, we wish to draw upon the phenomenological similarities between the ARPES data for LSCO and Bi2212 along $(0,0)$ to (π, π) . Empirically, ARPES features along $(0,0)$ to (π, π) are always sharp, even in underdoped materials (Fig. 1e-f). This is also the case for YBCO and Bi2212 systems [39] [56] [57] [58] as well as the insulating $\text{Sr}_2\text{CuO}_2\text{Cl}_2$ and $\text{Ca}_2\text{CuO}_2\text{Cl}_2$ [59]. The only cuprate that violates this empirical rule is the LSCO system. The data from LSCO system show strong resemblances to

that of the Zn doped system here [60]. In the LSCO case spectra along the $(0,0)$ to (π, π) direction are found to be extremely broad, while one can still see well defined peaks near $(\pi, 0)$ for highly doped cases - a fact that shows that the extremely broad feature along the $(0,0)$ to (π, π) direction is not due to a bad surface. With the increase of Sr doping, the change of the spectra along $(0,0)$ to (π, π) is not monotonic. For $x < 0.05$, one sees a broad dispersive feature that behaves like the feature seen in the insulating $\text{Sr}_2\text{CuO}_2\text{Cl}_2$. For $0.05 < x < 0.15$, one hardly sees any dispersive feature at all. For $x > 0.2$ one again sees a dispersive feature that shows a clear Fermi level crossing. Hence, the broadness of the feature along $(0,0)$ to (π, π) is not simply due to the random disorder of the Sr impurities as the Sr content increases monotonically. There is another likely contribution to the broadness of the features, and the contribution might be connected to the intrinsic electronic inhomogeneity. Based on neutron experiments, the evidence for stripe correlation is strongest in the LSCO system and is most visible in the doping range near $\frac{1}{8}$ [19]. Given the similarity of the data from Zn doped Bi2212 and from LSCO, one may wonder whether the destruction of the spectral peak along $(0,0)$ to (π, π) in the Zn samples is also related to the electronic inhomogeneity. This issue is also related to the recent transport measurement on Zn-Y doped Bi2212 [31].

Extensive numerical calculations using Hubbard or t-J models have been carried out on small cluster samples [61]. The systematics of the spectral lineshapes seen in Bi2212, YBCO, $\text{Sr}_2\text{CuO}_2\text{Cl}_2$, $\text{Nd}_{2-x}\text{Ce}_x\text{CuO}_4$, as well as the doping dependence, can very well be accounted for by these calculations. However, the spectral behavior of Zn doped Bi2212 and LSCO cannot be explained by these calculations even qualitatively. All calculations produce a sharp structure along $(0,0)$ to (π, π) , even when additional parameters such as t' and t'' are included [62]. On the other hand, an exact diagonalization of the spectral function shows that an introduction of attractive forces along the $(\pi, 0)$ or $(0, \pi)$ directions strongly suppresses the quasiparticle-pole strength along $(0,0)$ to (π, π) direction [63]. These forces were introduced to simulate the effects of stripes on the electronic structure, although the origin of stripes is unclear. In another calculation on the t-J model, it is found that a Zn vacancy pins the domain wall, similar to the case where a Zn vacancy bounds a hole of $d_{x^2-y^2}$ symmetry [64]. Summarizing the above discussion, it appears that the scenario of electronic phase separation can provide a self consistent accounting of the data. However, the above interpretation is not unique, and the phase separated regions do not necessarily have 1D order.

Alternatively, the interpretation of the data may come from a more phenomenological viewpoint. Zn does have an effect on the electronic properties of the cuprates. One particular result is that Zn induces local moments on neighboring Cu sites [8] [65]. This glassy array of an-

tiferromagnetic droplets will probably become more ordered as the temperature is lowered [66]. This will affect the electronic structure, and it is possible that the phenomena here are just manifestations of that fact. At the same time, quasiparticles at $(\frac{\pi}{2}, \frac{\pi}{2})$ may suffer significant scattering, resulting in the washed out features we see here. The spectral lineshape changes at $(\pi, 0)$ are not surprising as Zn has an effect on the superfluid density, n_s . According to Nachumi *et al.* [67], the Zn impurity acts as a dead center for n_s . This pocket of no superfluid extends over an area of $\pi\xi^2$, where ξ is the in-plane coherence length. This also says that the volume available for superconductivity is reduced, and this ought to be reflected as a decrease in n_s . Comparing the relative strength of the $(\pi, 0)$ peak with and without Zn, it is hard to say that the data points towards this conclusion. Furthermore, one should compare samples with the same δ , and that has been a hard parameter to control in the growth of Bi2212. It should be noted that while we have included this for the sake of discussion, the role of Zn in forming local moments in underdoped cuprates is still an open issue [68].

The next issue concerns the spectral lineshape of the photoemission experiments. The systematic changes in ARPES data with Zn doping provide a new perspective on several long standing problems about the unusual photoemission lineshape observed in high T_c superconductors. These problems can best be illustrated by the spectral lineshape change at $(\pi, 0)$ above and below T_c , as shown in Fig. 2. As the temperature is lowered below T_c , a sharp quasiparticle peak emerges at the low energy edge of the broad normal state feature accompanied by a dip structure at higher energy. In Zn doped Bi2212 the dip is gone, but the peak persists and even gains intensity as it is broadened but with roughly similar height. It is often assumed that the sharp peak develops below T_c because of an increase in quasiparticle lifetime, which is independently measured in other experiments [69] [70]. The traditional interpretation of the peak and dip structure is associated with the electronic pairing mechanism [71]. In this case, the peak is the superconducting quasiparticle at gap energy Δ (for the case when the normal state quasiparticle peak is at the Fermi level) and the dip is caused by the suppression of the spectral weight between the energy Δ and 3Δ as the electronic medium itself is gapped. More recently, a phenomenological self-energy was proposed to explain the peak and the dip in a very similar spirit [72]. In both of these cases, the dip and the peak go hand in hand because they are manifestations of the same self-energy change.

The data from Zn doped Bi2212 add to a list of puzzles associated with the above interpretation as Zn doping kills the dip without diminishing the intensity of the peak so that the peak and dip do not necessarily follow each other. The other puzzles are represented by the following examples. First, the expectation of spec-

tral weight suppression between Δ and 3Δ is based on a very general argument compatible with any electronic pairing mechanism so that the dip will appear as long as the electronic excitation spectrum opens a gap. This expectation is in strong contrast to the fact that one does not see a dip structure in the pseudogap state of the underdoped samples where the electronic excitation spectrum opens a gap [35]. It is also very strange that the sharp peak emerges only below T_c in the underdoped samples although the spectrum is gapped well above T_c , as if the single particle spectral function is sensitive to the superconducting order. Further, the intensity of the sharp peak shows a monotonic correlation with doping and, thus, the superfluid density. These empirical observations are not compatible with the conventional wisdom that the single particle spectral function should not be sensitive to the superconducting condensate. In fact, we believe this puzzle is a very important clue and its understanding will lead to a deeper insight into these materials. Second, the sharp peak and the broad feature at higher binding energy side of the dip seem to behave independently [73]. Fig. 2 shows the $(\pi, 0)$ spectra in the superconducting state with different doping. It is clear that the energy of the superconducting peak hardly changes, but the broad feature and the shape of the dip change significantly. Third, the photoemission spectra obtained in the normal state of the doped superconductor show a striking resemblance to that of the insulator, albeit the energy position of the broad feature near $(\pi, 0)$ evolves with different doping. Finally, we have to consider the fact that the peak and dip structures are not seen in YBCO. Despite the chain complication, we can still get the consistent result about the Fermi surface, the d-wave gap, and the sharp peak at X $(\pi, 0)$ in YBCO [39]. However, the dip structure is not seen even in measurements where the sample is cleaved and kept at 10K continuously. The above puzzles suggest that we may need to re-evaluate the problem in a very different way, as the conventional wisdom cannot explain the data.

IV. TEMPERATURE DEPENDENCE

In this section we report the temperature induced ARPES spectral change in Zn doped Bi2212. As with the spectra themselves, the temperature induced change varies with doping. With the increase of Zn impurities in the samples, we see a strong temperature dependence in the data. Furthermore, the temperature induced spectral change extends to very high energy in Zn doped samples. Empirically, the temperature dependence of the overdoped metal is much weaker than that of the underdoped insulator [74]. In the later case, the temperature dependence persists up to an energy scale of about an electron volt. Since the carrier density is not changed with Zn substitution of Cu, the enhanced temperature

dependence is consistent with the idea that Zn creates antiferromagnetic regions around it which exhibit stronger temperature dependence.

If Zn enhances the tendency of microscopic phase separation, the next question is whether the phase separation takes the form of 1D stripes as transport experiments seem to suggest [31]. The key difficulty lies in the fact that the traditional tools (*e.g.* X-ray or electron scattering) are sensitive to all electrons in the system, while the charge ordering, if present, occurs for electrons close to the Fermi level. This ‘large background’ signal from other electrons makes the detection of any charge density wave very difficult. Angle resolved photoemission may provide an opportunity to address this important and current issue as one can view ARPES as a kind of photoelectron diffraction experiment. Since the ARPES data near E_f probe only the last valence electron, it is naturally more sensitive to charge inhomogeneities as it discriminates against the background signal from other electrons. Further, the relatively low kinetic energy of these photoelectrons make them more sensitive to any charge density modulation than the high energy electrons and X-rays used in typical experiments. The complication, of course, is that these photoemitted valence electrons will be multiply scattered by other electrons (including the core electron) - a complex process itself is the source of information and, thus, cannot be avoided. This will reduce the sensitivity and increase the difficulty in the data analysis. Nonetheless, ARPES may still have higher sensitivity as it has the energy selectivity so one can probe specific orbitals.

Motivated by this consideration, we have made attempts to use ARPES to investigate the issue of charge stripes in cuprates. If charge stripes develop at low temperatures, as indirectly suggested by neutron scattering experiments, it may diffract the photoelectrons and cause a \mathbf{k} -dependent change in integrated spectral weight, $n(\mathbf{k})$. In an earlier report [42], we presented data that suggested a \mathbf{q} dependent spectral weight shift, and we have attributed that to the stripe instability because the \mathbf{Q} value so determined is quite close to what one expects from charge stripes. We have also observed the enhanced effect of the \mathbf{q} dependent spectral weight shift in the Zn doped samples. This latter aspect of the data, however, exhibits strong scatter and cannot be made unambiguous. Therefore, we have also detailed the uncertainties associated with our interpretation of the \mathbf{q} shift of the spectral weight and its connection with charge stripes. In this context, we have also discussed the claim that the spectral weight to be temperature independent [75]. We disagree with this premise and we show the prior data and claims of the same authors actually pointed to the contrary. We believe there are systematic changes of the spectra with temperature which depend on the doping and impurity concentration in the sample. On the other hand, the connection between the tempera-

ture dependence in the ARPES data and the stripe picture is not as straightforward as we have suggested [42], largely due to experimental uncertainties such as sample aging. Despite this, our recent work on Bi2212 systems has found a straight Fermi surface segment that strongly resembles the Fermi surface of the stripe phase in $\text{La}_{1.28}\text{Nd}_{0.6}\text{Sr}_{0.12}\text{CuO}_4$ [76]. This suggests that the charge stripe feature does exist in Bi2212, although the stripes are weaker as one can see the presence of quasiparticle like features near the d-wave node line. The quasiparticle state is strongly suppressed in Nd-LSCO where static stripes exist.

A. Experimental Observation

Fig. 3 shows ARPES data from pure and Zn doped samples. Again, two sets of data from Zn doped samples (Fig. 3d-e) were presented to illustrate reproducibility. Samples in Fig. 3a-b are pure Bi2212 sample while sample in Fig. 3c behaves as if it contains impurities. The first qualitative observation is that the Zn doped samples show a stronger temperature dependence. This temperature dependence correlates with the change of the spectral lineshape, with the Zn doped samples having a larger steplike background relative to the broad peak. As the temperature is lowered, a sharp peak develops near $(0.8\pi, 0) - (\pi, 0)$, but without a dip structure (Fig. 2a). The temperature induced change persists to very high energy. This is more clearly visible in the spectral lineshape of the sample in Fig. 3d. When the peak moves away from E_f , the spectra for the two temperatures have different curvatures, with the 100K spectra being concave down and the 20K spectra being concave up. This behavior is beyond experimental uncertainties as we will discuss later. The enhanced temperature dependence with Zn doping is consistent with the empirical result that the temperature dependence of ARPES gets stronger as the magnetic correlations get stronger. In $\text{Sr}_2\text{CuO}_2\text{Cl}_2$ we see a much stronger temperature dependence on an energy scale of approximately 1eV [74]. $\text{Sr}_2\text{CuO}_2\text{Cl}_2$ is a Mott insulator with strong magnetic correlation. In addition, the charge ordered manganite, $\text{Pr}_{0.5}\text{Sr}_{0.5}\text{MnO}_3$ shows a temperature dependence of spectral weight up to 1.2eV [77]. To contrast, overdoped Bi2201 (the one plane version of Bi2212) with weak magnetic correlation does not show much temperature dependence (see next paragraph). If Zn induces a local antiferromagnetic region around itself, it will presumably show a strong temperature dependence. This lends itself to the idea that Zn strengthens the tendency of microscopic phase separation.

We now move to the second aspect of the temperature dependence of the ARPES spectra from the Zn doped samples. While the spectral weight is gained near $(\pi, 0)$, it is reduced near $(0.3\pi, 0) - (0.5\pi, 0)$. At first glance,

it appears there is a \mathbf{q} dependent spectral weight shift [42]. The data from the two Zn doped samples are quite consistent with each other although they do differ in subtle ways. Judging from the sharpness of the feature, the sample in Fig. 3e is more overdoped than sample in Fig. 3d. As shown before, ARPES lineshapes are extremely sensitive to doping changes [35] [36]. To check whether the apparatus worked appropriately, we show in Fig. 4 ARPES data recorded at 20K and 100K for two Bi2201 samples taken under identical conditions as those of Bi2212 samples. As the temperature is lowered, the two sets of data match to within our error. In our experimental runs we checked the Bi2201 many times; the fact that they matched so well in all cases gave us confidence that the experimental apparatus worked properly. It is important to note that the calibration run using Bi2201 was not done across the superconducting transition so no significant lineshape change was involved and the situation was simpler.

While samples in Fig. 3a-b do not show any change in $n(\mathbf{k})$ with temperature, samples in Fig. 3c,d,e show subtle changes. Fig. 5 depicts the integrated spectral weight, $n(\mathbf{k}) = \int A(\omega, \mathbf{k}) f(\omega) d\omega$ versus $|\mathbf{k}|$ for the samples in Fig. 3b,c,d. Note that the $n(\mathbf{k})$ curves have different shapes so the change cannot be simply corrected by a shift in \mathbf{k} (or a tilt in angle) meaning the difference cannot be trivially attributed to angular irreproducibility with temperature. This point will be elaborated upon in detail later. Taken naively, it appears that the spectral weight is shifted from $\mathbf{k} \sim (0.3\pi, 0) - (0.5\pi, 0)$ to $(0.8\pi, 0) - (\pi, 0)$ region with a $|\mathbf{Q}|$ of about $0.4\pi - 0.5\pi$.

B. Discussion of Temperature Dependence Results

Because the \mathbf{Q} value of $(0.4\pi, 0) \sim (0.5\pi, 0)$ is quite similar to what one expects from stripes, we attributed this \mathbf{q} shift to the stripe instability [42]. We were further encouraged by the fact that the \mathbf{q} shift is more pronounced in Zn doped samples because Zn doping presumably enhanced the $\frac{1}{8}$ anomaly. This is also consistent with the fact that the spectra along $(0,0)$ to (π, π) direction of Zn doped samples look like that of LSCO where the evidence for stripes is the strongest [19] [22]. However, there are some important points to be addressed within that interpretation.

One important issue is whether this effect of a change in $n(\mathbf{k})$ was due to angular misalignment on our part. It is emphatically stated that our results were reproducible and exhaustively studied. The following statements are included to emphasize resoundingly the veracity of the qualitative aspect of this observation if not the quantitative as well. For the sake of argument, it is conjectured that the variation in $n(\mathbf{k})$ is due to some angular mismatch in going from above T_c to below T_c . To explore this possibility, we utilized an ARPES system with

finer momentum (angular) resolving power than previously used. The difference is at least a factor of *seven* better than that for the typical ARPES system. The resulting data (taken in angle mode) is presented for a $\text{Bi}_2\text{Sr}_2\text{Ca}(\text{Cu}_{0.99}\text{Zn}_{0.01})_2\text{O}_{8+\delta}$ sample in Fig. 6. Data is presented for both an aged and a fresh sample. It is noted that no pair of hot and cold curves overlay each other, that is to say, assuming some kind of angular misalignment in cooling the apparatus, one would expect a given high temperature curve to have some match among the group of cooler curves. That is not the case. A realistic question would be if sample aging contributed to this effect. It is noted that the intentionally aged sample also has no pair of matching curves. Now, of course, thermal broadening must be taken into account as well as the fact that there is some amount of change due to the superconducting state *especially* near $(\pi, 0)$. However, the points chosen were not close to $(\pi, 0)$ and thermal broadening of this magnitude does not account for the differences seen. To investigate this even further, the spectral weight was integrated for both samples and plotted versus \mathbf{k} in Fig. 7. The data from the fresh Zn sample reproduces the results of Fig. 3 and Fig. 5 and are consistent with our earlier results [42]. The reader can readily discern that in the very least, the shapes of the $n(\mathbf{k})$ do not match one another, either for the fresh or aged sample, no matter how they are translated in \mathbf{k} (an action correcting for the supposed angular misalignment). Although the interpretation of the data may change in light of new findings or information, the experimental observation of this effect is without question.

An additional issue to be addressed concerns periodicity of the \mathbf{Q} structure. A central premise in solid state physics is that periodicity seen in the first Brillouin zone at \mathbf{q} should also be seen at $\mathbf{q}+\mathbf{G}$ in the second Brillouin zone, where \mathbf{G} is the usual reciprocal lattice vector. That is to say that the effect we found between $[0, \pi]$ should be realized between $[\pi, 2\pi]$ as well. This observation would confirm our estimate of $|\mathbf{Q}|$ and establish a true periodicity. However much this is desired, the experiment, nonetheless, dictates its impracticality. This would involve the sampling of more points, which would increase the likelihood of aging effects, which have been so detrimental to the experimental act. However, in an attempt to satisfy a probable and fair question on the part of the reader, we utilized our system at ALS with the higher photon flux and sampling density. Our results on a Zn doped sample are shown in Fig. 8 as an $n(\mathbf{k})$ plot extending into the second Brillouin zone. What this plot shows is the suppressed spectral weight between $[\pi, 2\pi]$. This is most likely due to matrix element effects [43]. The error bars in the second zone comprise a larger percentage of the total as compared to the first zone. Taking a difference of these above and below T_c would be less informative than doing so in the first zone, and we are already pushing the experimental limitations of our ap-

paratus. It is possible to revisit this question.

It has been recently been suggested that $n(\mathbf{k})$ should be temperature *independent*. Further, all temperature induced changes are confined in the window of 3Δ with Δ being the superconducting gap [43]. Following that assumption, any temperature dependence ought to be attributable to experimental artifact. However, after careful consideration of some key results, we find the assertion of spectral weight conservation to be inconsistent. Fig. 9 reproduces data [43] published by the same authors cited in ref. 75 as a proof for the lack of temperature dependence [43]. In ref. 43, in distinct contrast to ref. 75, the same authors state that spectral weight *is* conserved for $\mathbf{k}=\mathbf{k}_f$ but *is not* conserved for $\mathbf{k}\neq\mathbf{k}_f$ (which is the region of relevance). After subtracting out temperature dependent background, the same authors claimed a 10% change in spectral weight between $T=13\text{K}$ and $T=105\text{K}$. While the reason for this inconsistency of claims by the same authors needs to be investigated, it is clear that the claim of spectral weight conservation has not been established contrary to ref. 75.

Some other points are in order concerning the issue of angular misalignment [75]. The $n(\mathbf{k})$ curves (see Fig. 5 and Fig. 7) show shape changes with temperature that cannot be explained by a rigid angular shift, as discussed earlier. In other words, one cannot slide the two $n(\mathbf{k})$ curves at different temperatures to match each other because they have different shapes, contrary to the example of ref. 75. As shown by the results of Fig. 4, the experimental setup works appropriately. The fact that the spectra at two temperatures match so well in the Bi2201 samples in all cases rule out the possibility of angle tilt of our sample manipulator as the temperature changed. Any possible angle shift can only stem from the mechanical flatness of the sample surface which is a random quantity. However, we have observed a strong correlation between the \mathbf{q} shift and other electronic structure changes: the destruction of the normal state quasiparticle along the (π, π) direction, the suppression of the superconducting gap, the broadening of the superconducting peak, and the suppression of the superconducting dip near $(\pi, 0)$. While the surface flatness can introduce error, this random variable alone cannot explain the *systematic* changes observed.

To further test the issue of charge stripes in Bi2212, we need to find a better way to passivate the surface. Although Bi2212 has a very stable surface in comparison to most cuprate samples, it appears that it is not stable enough if one wants to detect very subtle effects on the scale of a few percent unless extreme care is taken with respect to vacuum quality. This is the main source of uncertainty of our previous result [42]. Rather than wrestle further with this uncertainty, perhaps an alternative methodology would serve. To test the idea of stripes, we need to study materials where the evidence for stripes from other experiments is unambiguous (this

will establish what one should expect from stripes, although some theoretical ideas have already been proposed). This has been done recently in the stripe phase of $\text{La}_{1.28}\text{Nd}_{0.6}\text{Sr}_{0.12}\text{CuO}_4$ [78]. The effect is very strong so a modulation of $n(\mathbf{k})$ with 0.5π periodicity is seen without the need to do the difference curve. More recently, we have used an alternative approach to the problem by looking at the Fermi surface nesting feature which is strongly present in the stripe phase [78]. With a global mapping in $n(\mathbf{k})$, we have found clear Fermi surface nesting features similar to those seen in the static charge order phase [76]. This does support the notion of the presence of stripes even in Bi2212 when one looks at the data with high frequency. However, the stripe instability is weaker in Bi2212 than in the LSCO system. In Bi2212, one can still see a quasiparticle like feature along (π, π) direction while this is totally absent in LSCO.

V. SUMMARY

In conclusion, we recast the most important qualitative observation of our experiment - the destruction of the quasiparticle peak along ΓY with relatively small amounts of Zn impurities. Whatever the microscopic mechanism causing the change, be it simple impurity scattering or some random pinning of the phase separated domains, this observation is significant to the understanding of the relevance of quasiparticles in the normal state. Data in Fig. 1a,b,e,f may reasonably be interpreted within the context of the quasiparticle picture, a concept that is the foundation of the modern theory of solids and is extensively used to address the high T_c problem. Yet, one would be very hard pressed to call the data in Fig. 1c-d as reflecting quasiparticles, and superconductivity with T_c as high as 83K survived. Taken naively, the existence of conventional quasiparticles with well defined \mathbf{k} does not seem to be necessary for the realization of high temperature superconductivity. We also have studied temperature dependence in the ARPES data from the $\text{Bi}_2\text{Sr}_2\text{Ca}(\text{Cu}_{1-x}\text{Zn}_x)_2\text{O}_{8+\delta}$ system. With Zn doping, we observed strong temperature dependence in the data which persists up to very high energy. This observation is consistent with the idea that Zn enhances the tendency of electronic inhomogeneity, a result consistent with NMR result [8].

We acknowledge S.A. Kellar, X.J. Zhou, and P. Bogdanov for technical help, and R.B. Laughlin, D. S. Dessau, A.J. Millis, M. Norman, B.O. Wells, S.A. Kivelson, A. Fujimori, D. J. Scalapino, H. Eisaki, N. Nagosa, and D. van der Marel for helpful discussions. ARPES experiments were performed at SSRL which is operated by the DOE Office of Basic Energy Science, Division of Chemical Sciences. The Office's Division of Material Science provided support for this research.

-
- [1] A. Maeda *et al.*, *Phys. Rev. B* **41**, 4112 (1990)
 - [2] G. Xiao *et al.*, *Phys. Rev. B* **42**, 8752 (1990)
 - [3] T.R. Chien, Z.Z. Wang, and N.P. Ong, *Phys. Rev. Lett.* **67**, 2088 (1991)
 - [4] Y. Fukuzumi *et al.*, *Phys. Rev. Lett.* **76**, 684 (1996)
 - [5] R. Lal *et al.*, *Phys. Rev. B* **49**, 6382 (1994)
 - [6] T. Kluge *et al.*, *Phys. Rev. B* **52**, R727 (1995)
 - [7] H. Hancotte *et al.*, *Phys. Rev. B* **55**, R3410 (1997)
 - [8] H. Alloul *et al.*, *Phys. Rev. Lett.* **67**, 3140 (1991)
 - [9] K. Ishida *et al.*, *Physica C (Amsterdam)* **179**, 29 (1991)
 - [10] J.W. Loram, *Physica C* **235-240**, 134 (1994)
 - [11] J.L. Tallon *et al.*, *Phys. Rev. Lett.* **79**, 5294 (1997)
 - [12] D.A. Bonn *et al.*, *Phys. Rev. B* **50**, 4051 (1994)
 - [13] K. Mizuhashi *et al.*, *Phys. Rev. B* **52**, R3884 (1995)
 - [14] S. Tajima, R. Hauff, and W.-J. Jang, *SPIE* **2696**, 24 (1996)
 - [15] C. Bernhard *et al.*, *Phys. Rev. Lett.* **77**, 2304 (1996)
 - [16] H. Hirota *et al.*, *Physica B* **241-243**, 817 (1997)
 - [17] K. Kakurai *et al.*, *Phys. Rev. B* **48**, 3485 (1993)
 - [18] Y. Sidis *et al.*, *Phys. Rev. B* **53**, 6811 (1996)
 - [19] J.M. Tranquada, cond-matt/9709325; J.M. Tranquada *et al.*, *Nature* **375**, 561 (1995)
 - [20] K. Yamada *et al.*, *Phys. Rev. B* **57**, 6165 (1998); T. Suzuki *et al.*, *Phys. Rev. B* **57**, R3229 (1998); H. Kimura *et al.*, preprint
 - [21] N.L. Wang *et al.*, *Phys. Rev. B* **57**, R11081 (1998)
 - [22] Y. Koike *et al.*, *Solid State Communication* **82**, 889 (1992); Y. Koike *et al.*, *Physica C* **282-287**, 1233 (1997); Y. Koike *et al.*, *Journal of Low Temp. Phys.* **105**, 317 (1996); M. Akoshima *et al.*, *Phys. Rev. B* **57**, 7491 (1998)
 - [23] P. Dai, H.A. Mook, and F. Dogan, *Phys. Rev. Lett.* **80**, 1738 (1998); H.A. Mook *et al.*, *Phys. Rev. Lett.* **77**, 370 (1996)
 - [24] V.J. Emery, S.A. Kivelson, O. Zachar, *Phys. Rev. B* **56**, 6120 (1997)
 - [25] G. Siebold *et al.*, *Phys. Rev. B* **58**, 13506 (1998)
 - [26] J. Zaanen and O. Gunnarson, *Phys. Rev. B* **40**, 7391 (1989)
 - [27] H. J. Schultz, *J. Phys. (Paris)* **50**, 2833 (1989)
 - [28] A.H. Castro Neto and F. Guinea, *Phys. Rev. Lett.* **80**, 4040 (1998)
 - [29] Yu. A. Krotov, D.-H. Lee, and A.V. Balatsky, *Phys. Rev. B* **56**, 8367 (1997)
 - [30] S.R. White and D.J. Scalapino, *Phys. Rev. Lett.* **80**, 1272 (1998); *ibid.* **81**, 3227 (1998)
 - [31] M. Akoshima *et al.*, *Phys. Rev. B* **57**, 7491 (1998)
 - [32] C.G. Olson *et al.*, *Science* **245**, 731 (1989)
 - [33] Z.-X. Shen *et al.*, *Phys. Rev. Lett.* **70**, 1553 (1993)
 - [34] D.S. Marshall *et al.*, *Phys. Rev. Lett.* **76**, 4841 (1995)
 - [35] A.G. Loeser *et al.*, *Science* **273**, 325 (1996)
 - [36] H. Ding *et al.*, *Nature* **382**, 51 (1996)
 - [37] C. Quitmann *et al.*, *Phys. Rev. B* **53**, 6819 (1996); C. Quitmann *et al.*, *Journal of Superconductivity* **8**, 635 (1995); P. Almeras *et al.*, *Solid State Communications* **91**, 535 (1994); P. Almeras *et al.*, *Physica C* **235-240**, 957 (1994)

- [38] C. Gu *et al.*, *J. Phys. Chem. Solids* **54**, 1177 (1993)
- [39] M.C. Schabel *et al.*, *Phys. Rev. B* **55**, 2796 (1997); M.C. Schabel *et al.*, *Phys. Rev. B* **57**, 6107 (1998); M.C. Schabel *et al.*, *Phys. Rev. B* **57**, 6090 (1998)
- [40] R. Yoshizaki *et al.*, *J. Low Temp. Phys.* **105**, 927 (1996); D.-S. Jeon *et al.*, *Physica C* **253**, 102 (1995); L.-X. Chen, H. Ikeda, and R. Yoshizaki, *Physica C* **282-287**, 1205 (1997)
- [41] G.D. Gu *et al.*, *J. Crystal Growth* **137**, 472 (1994); G.D. Gu *et al.*, *J. Crystal Growth* **130**, 325 (1993); G.D. Gu *et al.*, *Physica C* **263**, 180 (1996)
- [42] Z.-X. Shen *et al.*, *Science* **280**, 259 (1998)
- [43] M. Randeria *et al.*, *Phys. Rev. Lett.* **74**, 4951 (1995)
- [44] H. Ding *et al.*, *Phys. Rev. Lett.* **78**, 2628 (1997)
- [45] In this paper we follow the conventional notation in the literature and call the broad peak seen in the normal state the quasiparticle peak. More critical analysis of the normal state data, especially the contrast between the normal and superconducting states at $(\pi, 0)$, suggests that one may not be able to meaningfully describe a quasiparticle peak in the normal state, at least for the \mathbf{k} -space region away from the $(0,0)$ to (π, π) line. (G.A. Sawatzky, private communication)
- [46] The low temperature data does allow the possibility of a gap, but more needs to be done before a conclusion can be drawn.
- [47] D.S. Dessau *et al.*, *Phys. Rev. Lett.* **66**, 2160 (1991)
- [48] Y. Hwu *et al.*, *Phys. Rev. Lett.* **67**, 2573 (1991)
- [49] V.J. Emery, S.A. Kivelson, *Nature* **374**, 4347 (1995)
- [50] S. Doniach, M. Inui, *Phys. Rev. B* **41**, 6668 (1990)
- [51] C.S. de Melo, M. Randeria, J.R. Engelbrecht, *Phys. Rev. Lett.* **71**, 3202 (1993)
- [52] K. Morikawa *et al.*, *Phys. Rev. B* **54**, 8446 (1996)
- [53] M. Hase *et al.*, *J. Magn. Magn. Mat.* **177-181**, 611 (1998)
- [54] K. Manabe *et al.*, *Phys. Rev. B* **58**, R575 (1998)
- [55] T. Sekine *et al.*, *J. Phys. Soc. Japan* **67**, 1440 (1998)
- [56] R. Liu *et al.*, *Phys. Rev. B* **45**, 5614 (1992); R. Liu *et al.*, *Phys. Rev. B* **46**, 11056 (1992)
- [57] J.M. Harris *et al.*, *Phys. Rev. B* **54**, R15665 (1996)
- [58] K. Gofron *et al.*, *Phys. Rev. Lett.* **73**, 3302 (1994)
- [59] B.O. Wells *et al.*, *Phys. Rev. Lett.* **74**, 964 (1995)
- [60] A. Ino *et al.*, cond-mat/9809311
- [61] E. Dagatto, *Rev. Mod. Phys.* **66**, no. 3, 763 (1994)
- [62] C. Kim, *et al.*, *Phys. Rev. Lett.* **80**, 4245 (1998)
- [63] T. Tokyama and S. Maekakwa, private communication
- [64] D. Poilblanc, D.S. Scalapino, W. Hanke, *Phys. Rev. Lett.* **72**, 884 (1994)
- [65] A. V. Mahajan *et al.*, *Phys. Rev. Lett.* **72**, 3100 (1994)
- [66] C. Pepin and P. A. Lee, *Phys. Rev. Lett.* **81**, 2779 (1998)
- [67] B. Nachumi *et al.*, *Phys. Rev. Lett.* **77**, 5421 (1996)
- [68] G. V. M. Williams and J. L. Tallon, *Phys. Rev. B* **57**, 10984 (1998); C. Bernhard *et al.*, *Phys. Rev. Lett.* **58**, R8937 (1998)
- [69] D.A. Bonn, *et al.*, *Phys. Rev. Lett.* **68**, 2390 (1992)
- [70] J.M. Harris, *et al.*, *J. Low Temp. Phys.* **105**, 877
- [71] P.B. Littlewood and C. M. Varma, *Phys. Rev. B* **45**, 12636 (1992)
- [72] M.R. Norman and H. Ding, *Phys. Rev. B* **57**, R11089 (1998)
- [73] Empirically, one may naively think that the peak and dip minimum energy actually scale with each other. This is reasonable as the dip minimum energy is basically determined by the peak energy and half of the width.
- [74] C. Kim *et al.*, unpublished
- [75] J.C. Campuzano *et al.*, cond-matt/9811349
- [76] D. Feng *et al.*, unpublished
- [77] A. Chainani *et al.*, *Phys. Rev. B* **56**, R15513 (1997)
- [78] X.J. Zhou, P. Bogdanov, S.A. Kellar, T. Noda, H. Eisaki, S. Uchida, Z. Hussain, Z.-X. Shen, *Science* **286**, 268 (1999)

FIG. 1. ARPES data along $(0,0)$ to (π,π) cut for several types of $\text{Bi}_2\text{Sr}_2\text{CaCu}_2\text{O}_{8+\delta}$. The number near the spectrum indicates the \mathbf{k} -space point. (a) and (b) are pure with T_c of 91K; (c) and (d) are Zn doped with T_c of 83K; (e) is 10% Dy doped with T_c of 65K (underdoped sample); (f) is an oxygen reduced (underdoped) with T_c of 67K. All spectra were collected at 100K under comparable conditions. For the Zn doped sample (d), spectra recorded below T_c (gray line) is the same within the experimental uncertainty. The topmost spectrum in panel (a) is the *average* of the others (see text for discussion).

FIG. 2. ARPES spectra of $\text{Bi}_2\text{Sr}_2\text{CaCu}_2\text{O}_{8+\delta}$ recorded at $(\pi,0)$ for (a) pure ($T_c \approx 91\text{K}$) and Zn doped ($T_c \approx 83\text{K}$) in the normal (100K) and superconducting (20K) states and for (b) pure underdoped and overdoped in the superconducting state (20K).

FIG. 3. ARPES data along $(0,0)$ to $(\pi,0)$ cut for $\text{Bi}_2\text{Sr}_2\text{CaCu}_2\text{O}_{8+\delta}$ for (a) pure ($T_c \approx 89\text{K}$); (b) pure ($T_c \approx 91\text{K}$); (c) pure ($T_c \approx 88\text{K}$); (d) Zn doped ($T_c \approx 78\text{K}$); (e) Zn doped ($T_c \approx 83\text{K}$). 100K data are represented by the gray lines while 20K data are represented by the black lines.

FIG. 4. ARPES data along $\Gamma\bar{M}$ cut for two samples (a and b) of the overdoped version of the one plane compound, $\text{Bi}_2\text{Sr}_2\text{CuO}_6$, with $T_c \approx 8\text{K}$. 100K data are represented by the gray lines while 20K data are represented by the black lines.

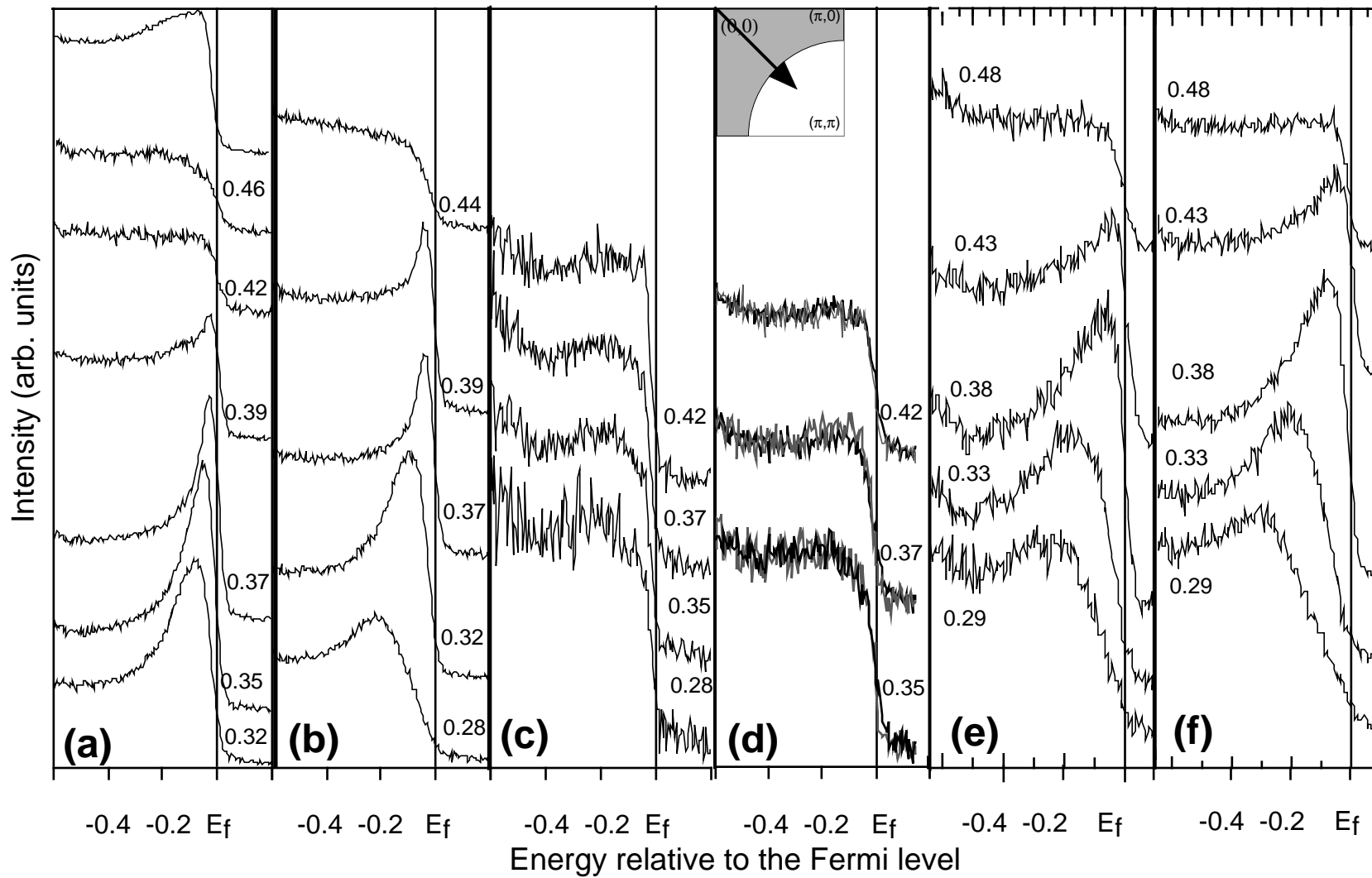
FIG. 5. $\text{Bi}_2\text{Sr}_2\text{CaCu}_2\text{O}_{8+\delta}$ $n(\mathbf{k})$ plots versus $|\mathbf{k}|$ for $(0,0)$ to $(\pi,0)$ for (a) pure ($T_c \approx 91\text{K}$, Fig. 3b); (b) pure ($T_c \approx 88\text{K}$, Fig. 3c); and (c) Zn doped ($T_c \approx 78\text{K}$, Fig. 3d). Open squares represent 100K data; filled circles represent 20K data. Error bars of $\pm 1\%$ of the total are not included because of scale.

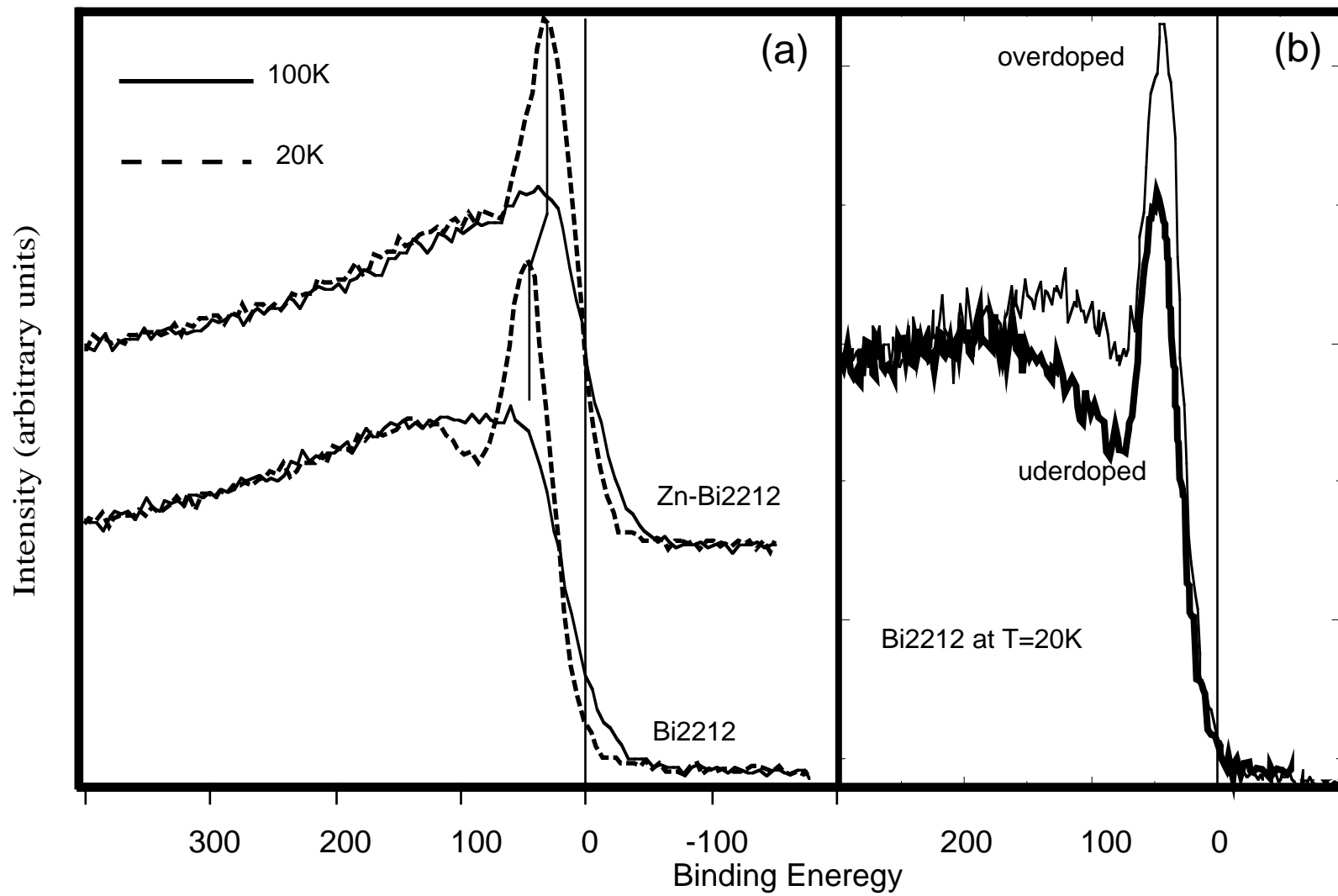
FIG. 6. Data from $\text{Bi}_2\text{Sr}_2\text{Ca}(\text{Cu}_{0.99}\text{Zn}_{0.01})_2\text{O}_{8+\delta}$ along $(0,0)$ to $(\pi,0)$ cut for $T=100\text{K}$ (solid), 20K (gray) for (a) fresh sample and (b) aged sample. The \mathbf{k} is indicated by the position along $(0,0)$ to $(\pi,0)$ in units of $\frac{\pi}{a}$ given by the number to the right for the topmost and bottom spectra. Successive pairs of spectra are evenly spaced to show detailed evolution of the features. Data are taken in angle mode.

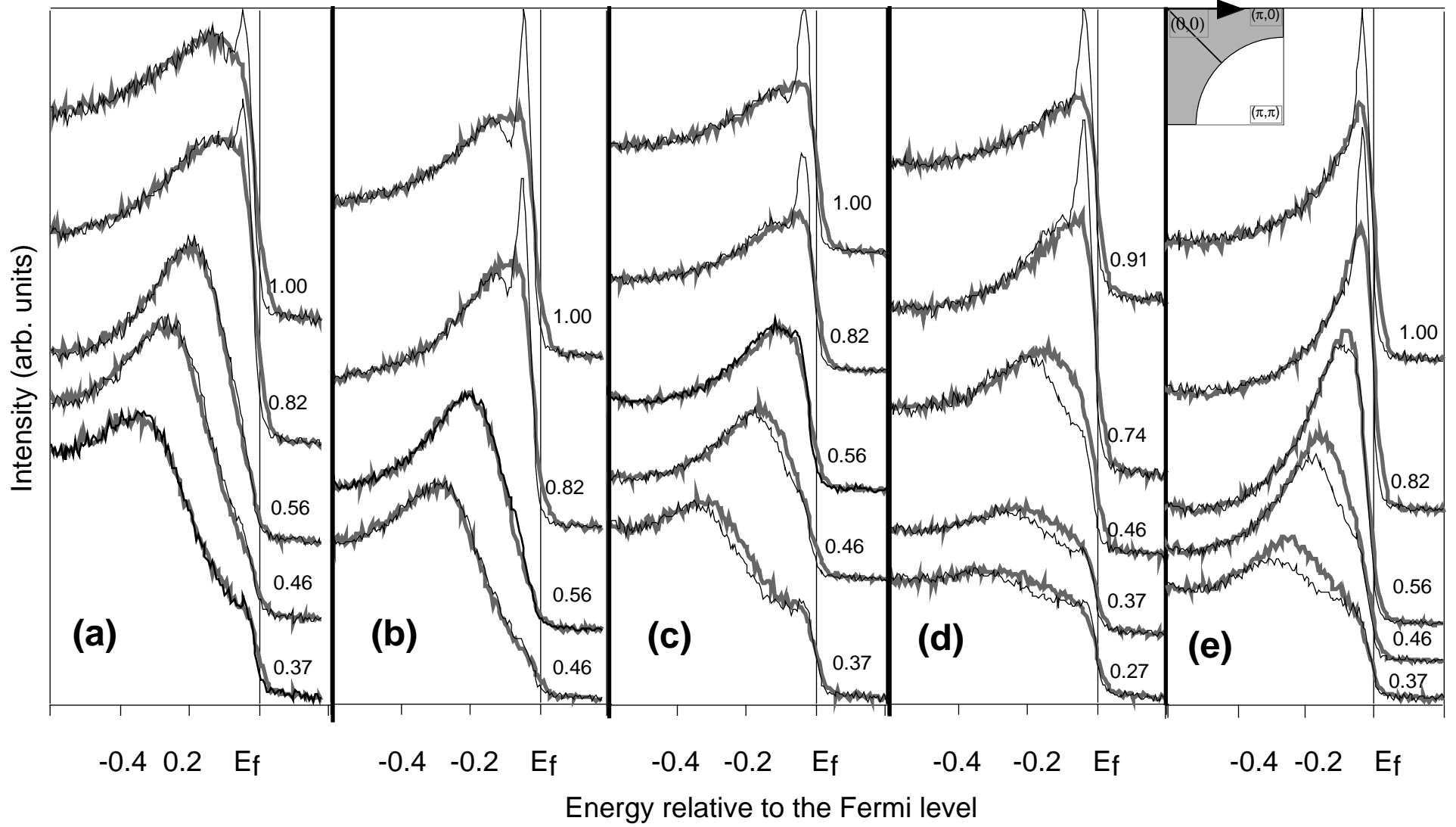
FIG. 7. (a) $n(\mathbf{k})$ plots along $\Gamma\bar{M}$ for fresh surface data (Fig. 6a). (b) $n(\mathbf{k})$ from aged surface data (Fig. 6b).

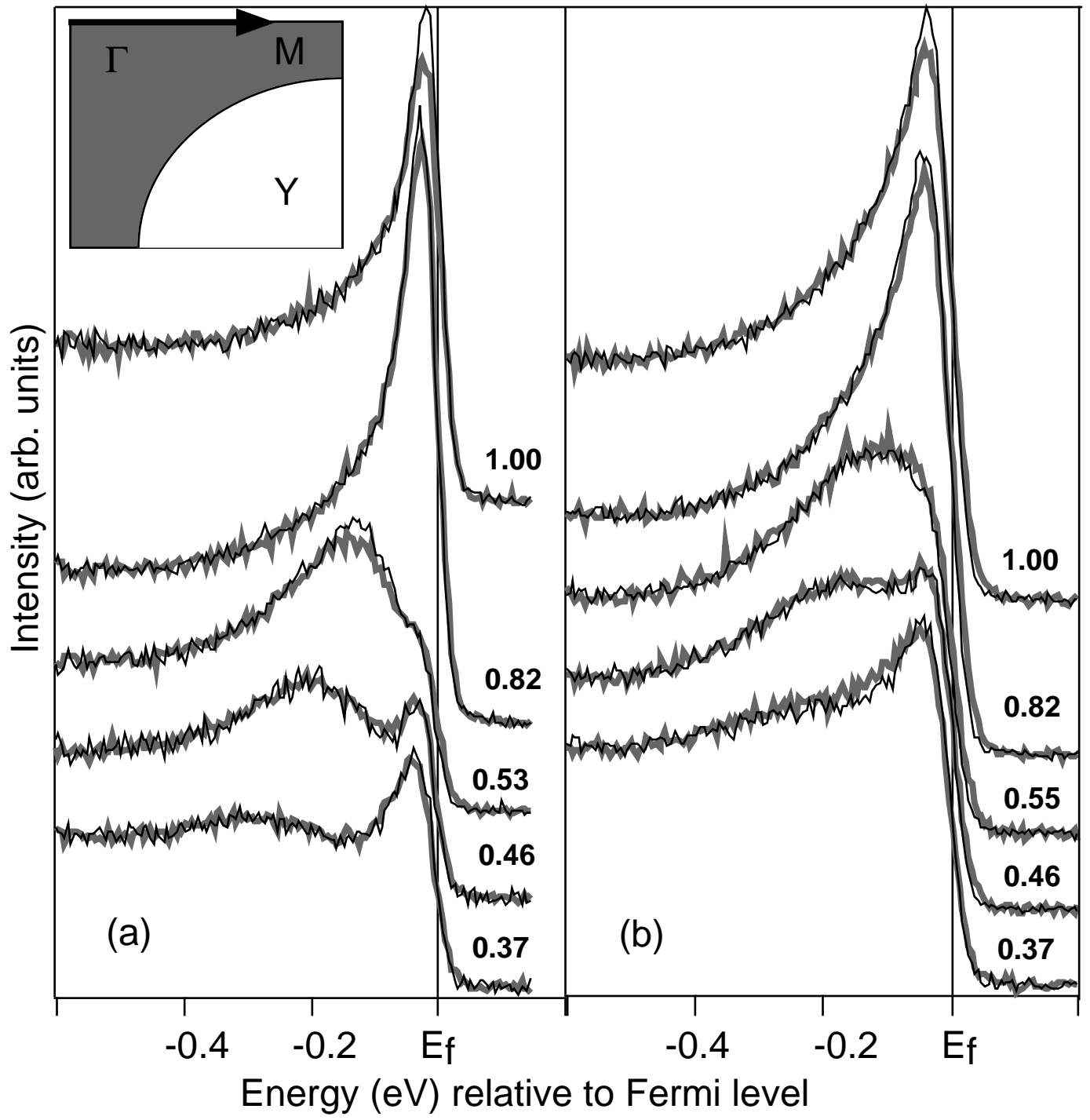
FIG. 8. $n(\mathbf{k})$ along $\Gamma\bar{M}$ for $\text{Bi}_2\text{Sr}_2\text{Ca}(\text{Cu}_{0.99}\text{Zn}_{0.01})_2\text{O}_{8+\delta}$ extending into the second Brillouin zone taken in the normal state ($T=100\text{K}$).

FIG. 9. Data taken from ref. 43 showing near optimal $\text{Bi}_2\text{Sr}_2\text{CaCu}_2\text{O}_{8+\delta}$ ($T_c \approx 87$) spectra near the \bar{M} point above (105K) and below T_c (13K).

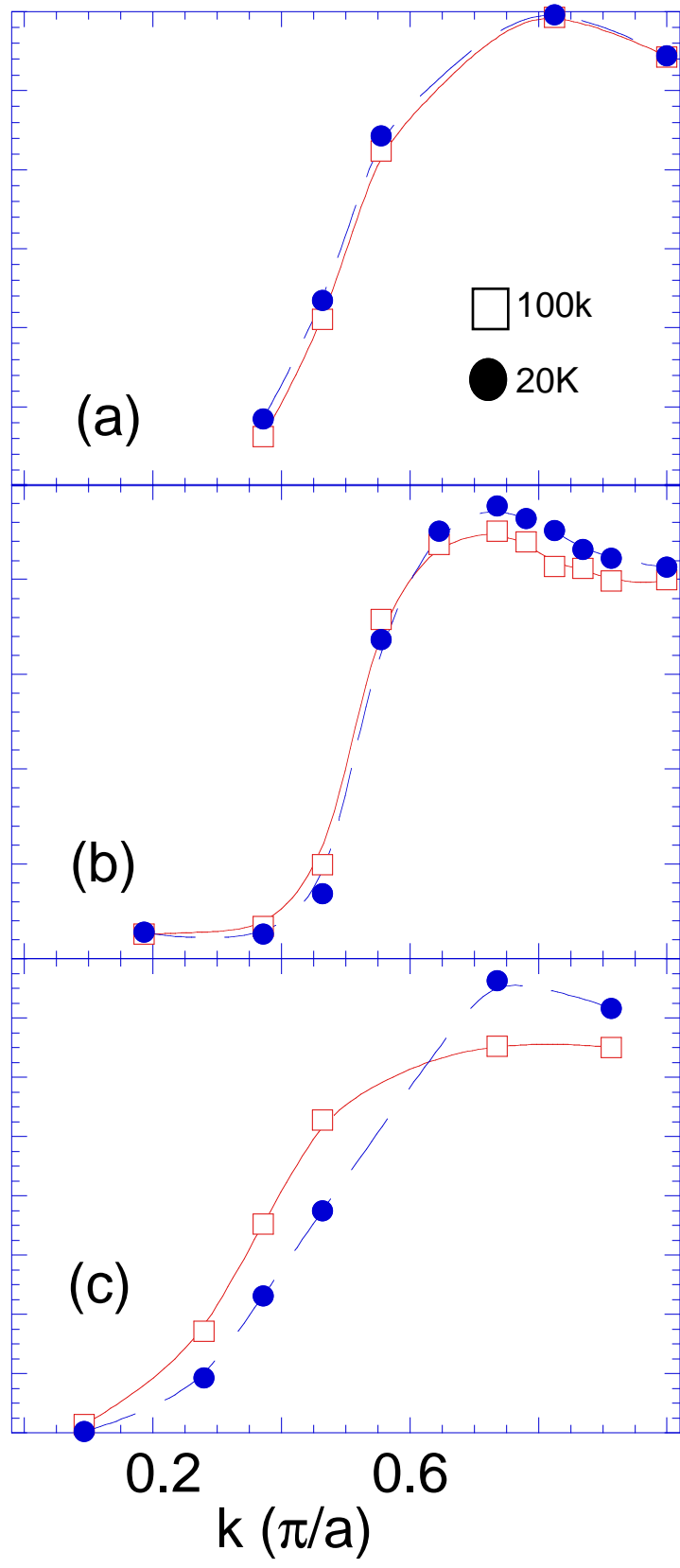




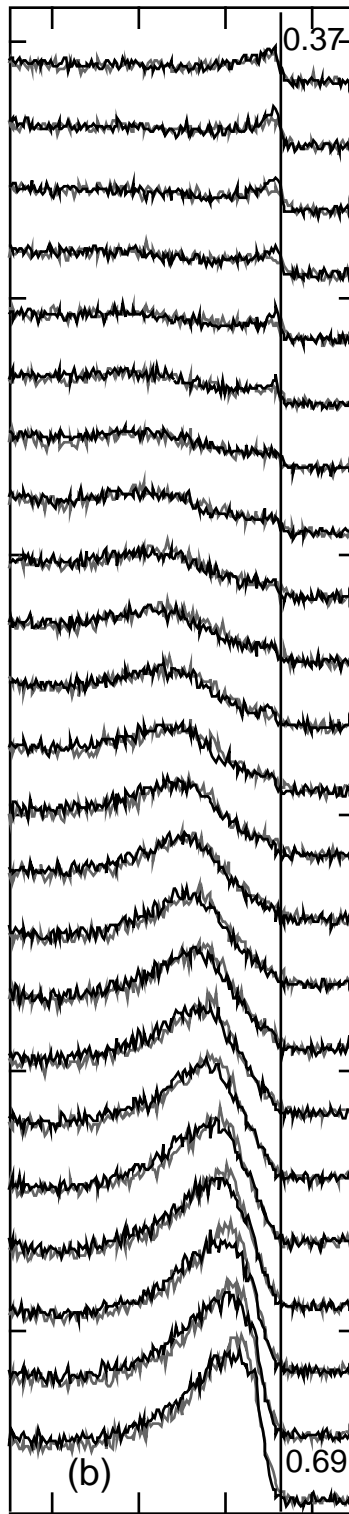
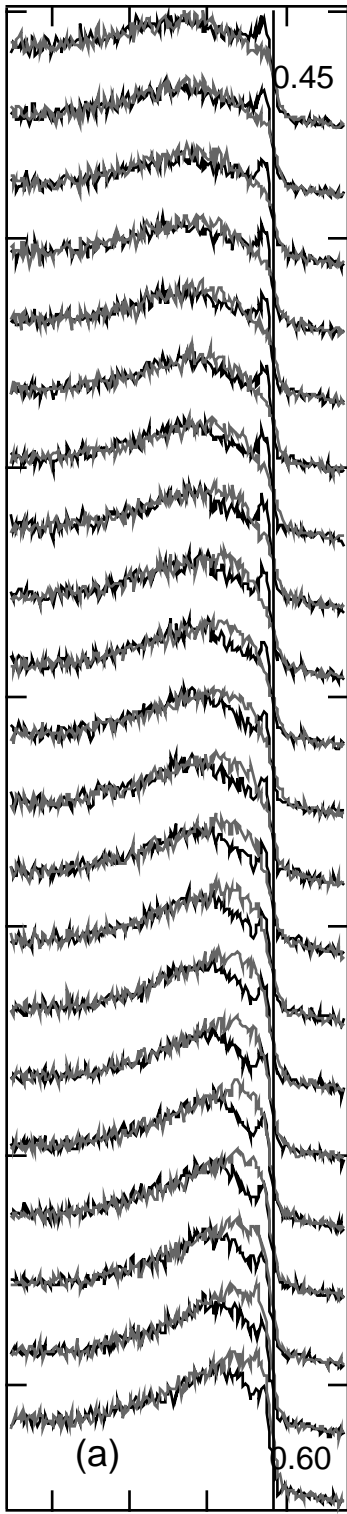




Integrated Intensity (arb. units)



Intensity (arb. units)



-0.56 -0.16 Ef

-0.52 0.12 Ef

Energy(eV) rel. to Fermi level

